Applied Catalysis B: Environmental 84 (2008) 426–432

Contents lists available at ScienceDirect

Applied Catalysis B: Environmental

journal homepage: www.elsevier.com/locate/apcatb

Selective oxidation of carbon monoxide over $CuO–CeO_2$ catalyst: Effect of hydrothermal treatment

Chang Ryul Jung [a], Arunabha Kundu [a,*], Suk Woo Nam [b], Ho-In Lee [c,*]

[a] Micro-fuel Cell Team, Electro Material and Device (eMD) Center, Corporate R&D Institute, Samsung Electro-Mechanics, 314 Maetan3-Dong, Yeongtong-Gu, Suwon, Gyunngi-Do 443-743, Republic of Korea
[b] Fuel Cell Research Center, Korea Institute of Science and Technology, Seoul 136-791, Republic of Korea
[c] School of Chemical and Biological Engineering and Research Center for Energy Conversion and Storage, Seoul National University, Seoul 151-744, Republic of Korea

ARTICLE INFO

Article history:
Received 10 April 2007
Received in revised form 22 April 2008
Accepted 24 April 2008
Available online 2 May 2008

Keywords:
$CuO–CeO_2$ catalyst
Hydrothermal treatment
Cu–Ce–O solid solution
Selective oxidation of CO
Phase separation
Copper
Ceria

ABSTRACT

Copper oxide–ceria ($CuO–CeO_2$) catalyst for selective oxidation of carbon monoxide (CO) was prepared by co-precipitation and hydrothermal treatment methods and evaluated for catalytic activity in a reformate gas composition which simulated the produced gas from methanol steam reforming. By applying the condition of hydrothermal treatment, the catalytic activity of $CuO–CeO_2$ catalyst was increased and the operating temperature window, in which the concentration of carbon monoxide was lower than 10 ppm, was widened. From the thermogravimetric (TG) results of hydrothermally treated catalyst precursor, $CuO–CeO_2$ catalyst did not show any improvement in physical properties such as Brunauer Emmett Teller (BET) surface area, pore volume and average pore diameter, but the chemical stability might be enhanced by hydrothermal treatment. By hydrothermal treatment, cuprous ion in the $CuO–CeO_2$ catalyst migrated to the surface of catalyst resulting in increased surface concentration of copper and formation of cupric oxide on the surface of catalyst during calcination. While increasing the calcination temperature (i.e. above 800 °C), the phase separation occurred with a part of copper and cupric oxide was formed on the surface of catalyst which was observed in X-ray diffraction (XRD) analysis.

1. Introduction

Among the various fuel cells, polymer electrolyte membrane fuel cell (PEMFC) is considered to be a technically advanced power generating system and it has several advantages, such as (i) low operating temperature, (ii) high power density, and (iii) rapid start up. While pure hydrogen is the best fuel for PEMFC, there are several limitations associated with the storage and distribution of hydrogen. A promising way to overcome these problems is to produce hydrogen on-board in a fuel-processing unit by directly converting a conventional fuel such as natural gas, gasoline or methanol to a hydrogen-rich gas mixture [1]. However, a small amount of carbon monoxide is present in the reformate gas and the presence of carbon monoxide (CO) gas may poison the Pt electrocatalyst that is generally used as an anode material in PEMFC. It is generally reported that the tolerance limit for carbon monoxide differs depending on type of anode catalyst materials. In the case of Pt anode catalyst which is more commonly used, the CO tolerance limit is less than 10 ppm [1–3], whereas for Pt–Ru alloy anodes, CO tolerance could be up to 100 ppm [4–6].

Among the various options available for reducing the CO concentration in the reformate gas such as the use of a separation membrane, methanation and selective oxidation of carbon monoxide, the last one with pure oxygen or air is undoubtedly the most straightforward, simplest and cost effective one [1,7]. In the last decade, many researchers have developed catalysts which can selectively oxidize carbon monoxide in the reformate gas.

The catalysts proposed for selective oxidation process are noble metal-based, such as alumina-supported platinum-group metal catalysts [7,8], zeolite-supported platinum catalysts [9], and metal oxide-supported gold catalysts [10–13]. Recently, $CuO–CeO_2$ oxide catalyst was proposed as a candidate for the selective oxidation of CO in the presence of excess hydrogen [14,15] because this catalyst is more active and selective than Pt-group-based catalysts at lower reaction temperature. In a previous study [16], it was found that

* Corresponding authors. Tel.: +82 2 880 7072; fax: +82 2 888 1604.
E-mail addresses: arunabhakundu@gmail.com (A. Kundu), hilee@snu.ac.kr (H.-I. Lee).

0926-3373/$ – see front matter © 2008 Elsevier B.V. All rights reserved.
doi:10.1016/j.apcatb.2008.04.024

$CuO–CeO_2$ catalyst prepared by co-precipitation method showed good activity and selectivity and the active site for selective oxidation of carbon monoxide in the catalyst was a Cu–Ce–O solid solution. More recent literature on the development of catalyst for selective oxidation of CO is provided in Table 1 [17–25]. These catalysts are mainly Pt-, Au- and CuO-based catalyst with various types of support materials like Al_2O_3, CeO_2, ZrO_2, SnO_2 and MnO_2. In addition Omata et al. [18] found $Co/SrCO_3$ with different additives like Bi, Ga and In as an effective catalyst for selective oxidation of CO. Lee et al. [21] synthesized Au/TiO_2 catalyst for selective oxidation of CO which is active at room temperature.

Hydrothermal synthesis at high temperature and high pressure using aqueous solutions and vapors reacting with solid materials is a well-known process in mineralogy and geology fields [26]. In particular, this synthesis method is suitable for the preparation of powder materials. Recent trends in the development of material synthesis techniques for the preparation of solid powders lead towards a more dispersed system [27] using solutions and/or gases as a starting material. The hydrothermal method is also used for crystal growth of compounds at a lower temperature. This method has the advantage of yielding high-quality crystals with less thermal strain at lower temperatures in comparison with other methods. However, few studies have reported on hydrothermal crystal growth of dielectric ceramic materials, e.g. Yanagisawa et al. [28].

In the present study, hydrothermal treatment is introduced in the development of catalyst for selective oxidation of carbon monoxide in order to increase the catalytic activity and enhance

Table 1
Recent literature on catalyst development for selective oxidation of CO

Authors	Type of catalyst	Operating conditions	Characteristics
Simsek et al. [17]	1% Pt–0.25% SnO_x and 1% Pt–1% CeO_x supported on activated carbon	Temperature: 150 °C Catalyst weight: 0.25 g Gas flow rate: 100 cm^3/min Gas composition: 1% CO, 1% O_2, 60% H_2, 15% CO_2 and inert He (balance) and 1% CO, 1% O_2, 60% H_2, 15% CO_2, 10% H_2O and inert He as balance	1% Pt–0.25% SnO_x catalyst supported on HNO_3-oxidized activated carbon gives 100% CO conversion and 1% Pt–1% CeO_x catalysts supported on the air-oxidized activated carbon gives 100% CO conversion
Omata et al. [18]	$Co/SrCO_3$_ with 10 different additives (B, K, Sc, Mn, Zn, Nb, Ag, Nd, Re, and Tl)	Temperature: 240 °C Catalyst weight: 0.12 g Gas flow rate: 1.5 g h/mol Gas composition: 1% CO, 0.5% O_2, 5% N_2 in H_2 and 0.73% CO, 0.36% O_2, 4.7% N_2, 18.0% CO_2, and 10.0% H_2O in H_2	The elements such as Bi, Ga, and In are better additive in $Co/SrCO_3$ catalyst 64% CO conversion and 70% selectivity for PROX with Co 3.2–Bi 0.3 mol%/$SrCO_3$
Gamarra et al. [19]	CuO/CeO_2 (1 wt% Cu and 5 wt% Cu)	Temperature: 25–250 °C Gas flow rate: 1.5 g h/mol Gas composition: 1% CO, 1.25% O_2 and 50% H_2 (Ar balance)	1 wt% Cu gives 100% CO conversion at 102 °C
Ayastuy et al. [20]	$MnO_x/Pt/Al_2O_3$	Temperature: 25–250 °C. Gas flow rate: 200 cm^3/min Gas composition: 1% CO, 0–60% H_2, 0–1.5% O_2, 0–5% CO_2, 0–5% H_2O and He (balance)	A maximum CO conversion of 89.8%, with selectivity of 44.9% and CO yield of 40.3% was obtained over a catalyst with 15 wt% Mn operating at 139 °C
Lee et al. [21]	Au/TiO_2	Temperature: room temperature 0–80 °C Catalyst weight: 0.04 g with 0.2 g silicon carbide Gas flow rate: 110 cm^3/min Gas composition: 1% CO, 50% H_2, 1% O_2, 48% N_2	The storage effect on catalytic activity was tested
Pozdnyakova et al. [22]	Pt/CeO_2 (1 wt% and 5 wt% Pt)	Temperature: 50–270 °C Catalyst weight: 0.082 g 1 wt% Pt/CeO_2 and 0.073 g of 5 wt% Pt/CeO_2 Gas flow rate: 100 cm^3/min Gas composition: 1% CO, 0.4–1% O_2 and the rest H_2	Mechanism of the PROX reaction on Pt/CeO_2 catalyst, using catalytic tests, in situ DRIFTS, high-pressure XPS, HRTEM, and TDS techniques
Son [23]	Ce-$Pt/\gamma–Al_2O_3$	Temperature: 100–350 °C Catalyst weight: 0.1–0.3 g Gas flow rate: 100 cm^3/min Gas composition: 1% CO, 0.5–1% O_2, 0–10.09% CO_2, 0–2.3% H_2O and the rest H_2	(a) Adding H_2O to the feed gas enhanced the CO conversion due to the water–gas shift reaction. (b) Adding CO_2 to the feed gas suppressed the CO conversion due to the reversible water–gas shift reaction
Avgouropoulos et al. [24]	Au/CeO_2 and CuO/CeO_2	Temperature: 50–250 °C Catalyst weight: 0.05–0.12 g Gas flow rate: 50–100 cm^3/min Gas composition: 1% CO, 1.25% O_2, 50% H_2, 0–15% CO_2, 0–10% H_2O and He as balance	Au/ceria catalysts showed higher activity than CuO/CeO_2 for the PROX reaction at temperatures lower than 120 °C, while the CuO/CeO_2catalysts were able to operate at higher tem peratures, with a remarkably better selectivity
Ayastuy et al. [25]	$Pt/Ce_XZr_{1-X}O_2$ (X = 0, 0.15, 0.5, 0.68, 0.8 and 1)	Temperature: 25–225 °C Gas flow rate: 200 cm^3/min Gas composition: 1% CO, 0–60% H_2, 0.5–1% O_2, 0–5% CO_2, 0–5% H_2O and He as balance	The catalyst with the composition of $Pt/Ce_{0.8}Zr_{0.2}O_2$, $Pt/Ce_{0.68}Zr_{0.32}O_2$ and $Pt/Ce_{0.5}Zr_{0.5}O_2$ shows complete CO conversion with effective oxygen use

the physical and chemical properties of the catalyst. Hydrothermally treated $CuO–CeO_2$ catalyst was prepared and evaluated for activity in the selective oxidation of carbon monoxide. The physical and chemical properties of hydrothermally treated $CuO–CeO_2$ catalyst was characterized through X-ray diffraction (XRD), X-ray photoelectron spectroscopy (XPS), temperature-programmed reduction (TPR) and CO chemisorption analysis.

2. Experimental

2.1. Preparation of catalyst

The $CuO–CeO_2$ mixed oxide was prepared by co-precipitation in an aqueous solution containing an excess NH_4OH, starting from a solution of $Cu(NO_3)_2{\cdot}3H_2O$ (Shinyo) and $Ce(NO_3)_3{\cdot}6H_2O$ (Kanto). The precipitate was filtered and washed several times with deionized water, then dried at 75 °C for 12 h. The precipitated powder was calcined at 700 °C under flowing air for 4 h.

After co-precipitation, the precipitate was transferred into a 0.0002-m^3 autoclave where hydrothermal ageing was performed at 240 °C for 12 or 24 h under water, nitrogen and oxygen medium in a batch system. In the autoclave, 0.0001 m^3 water was taken initially. After hydrothermal ageing, the solids were cooled to room temperature, then filtered and dried at 75 °C for 12 h. Finally, the solid powders were calcined at various temperatures under flowing air for 4 h. Three types of hydrothermally treated catalysts were prepared. The first one is the $CuO–CeO_2$ catalyst after the hydrothermal treatment for 12 h where the amount of CuO loading is 4.1 wt% (designated as HT-1 catalyst). The other two types are $CuO–CeO_2$ catalyst after the hydrothermal treatment for 24 h with the amount of CuO loading of 4.1 wt% (designated as HT-2 catalyst) and $CuO–CeO_2$ catalyst after the hydrothermal treatment for 12 h with the amount of CuO loading of 5.6 wt% (designated as HT-3 catalyst).

2.2. Characterizations

Thermogravimetric-differential thermal analysis (TG-DTA) of the catalyst precursor was carried out using a MAC Science TG-DTA 2000 thermal analyzer in the range of 30–1000 °C in air atmosphere. The heating rate was maintained at 5 °C/min.

Brunauer Emmett Teller (BET) surface area, pore volume and pore size distribution were measured by nitrogen adsorption–desorption at 350 °C using a Micromeritics ASAP 2010 instrument. Pore volume and pore size were determined by applying the Barrett–Joyner–Halenda method [29] to the desorption branch of the isotherm. Prior to the measurements, these samples were degassed at 200 °C for at least 2 h.

X-ray diffraction measurement was made using a Rigaku D/Max-IIIA X-ray diffractometer with a scan speed of 10°/min, in the scan range of 20–80° using Cu Kα as an X-ray source.

The mean crystallite size (D_β) of the CeO_2 grains was determined from line-broadening measurements on the ⟨1 1 1⟩ peak of CeO_2, using the Scherrer equation:

$$D_\beta = \frac{K\lambda}{\beta \cos\theta}$$

where λ is the X-ray wavelength, K is the particle shape factor, taken as 0.94 for spherical particles, β is the full-width at half maximum (FWHM) height in radians. The β-values were carefully determined by a least-square fit of a Gaussian function.

The TPR analysis was carried out using 5% hydrogen in argon as a reducing gas in a conventional TPR reactor. The description of the analysis was given elsewhere [30].

The XPS measurements were conducted using a Physical Electronics PHI 5800 with Al Kα radiation. The binding energies were corrected for the surface charge by referencing to C 1s peak of contaminant carbon at 284.5 eV. Deconvolution of the peak was performed with the best fitting routine of the XPSPEAK program.

In a Micromeritics ASAP 2010C apparatus, CO chemisorption analysis was performed with the same procedure as stated in Ref. [16].

2.3. Selective oxidation of carbon monoxide

The catalytic tests were carried out in a conventional fixed-bed and flow type reactor at atmospheric pressure. A quantity of 250 mg of catalyst and a total flow rate of the reaction mixture equal to 156 cm^3/min (W/F = 0.096 g s/cm^3) was used for each run. The reaction mixture consisted of 0.8% CO, 23.5% CO_2, 3.8% air, the balance being H_2.

A CO analyzer made by Siemens was used for the analysis of CO, CO_2 and O_2. Methane and hydrogen contents were analyzed by gas chromatography (Hewlett Packard 5890 series II) using a thermal conductivity detector (TCD). Methane was not detected under the present experimental conditions.

Catalytic activity was expressed by the conversion of CO or residual CO concentration. The CO conversion was calculated based on the CO consumption as follows:

$$\text{CO conversion}\,(\%) = \frac{[\text{CO}]_{\text{in}} - [\text{CO}]_{\text{out}}}{[\text{CO}]_{\text{in}}} \times 100$$

The calculation of CO conversion was based on the CO consumption only, because of the possibility of large error in the quantification of small changes in the CO_2 concentration.

3. Results and discussions

The amount of copper oxide loading in the prepared $CuO–CeO_2$ catalyst by co-precipitation was 4.1 wt% which was confirmed by atomic adsorption-induced coupled plasma (AA-ICP) analysis. In the case of HT-3 catalyst, the amount of copper oxide loading was 5.6 wt%.

To determine the calcination temperature of hydrothermally treated $CuO–CeO_2$ catalyst, TGA (thermogravimetry) analysis was carried out and the results are shown in Fig. 1. The weight loss for the $CuO–CeO_2$ catalyst prepared by co-precipitation method (CuO loading was 4.1 wt%) was 6 wt% whereas HT-1 catalyst decreased the weight loss by 4 wt% and the stabilizing temperature shifted to a lower value of about 100 °C. During the weight loss till 400 °C, no exothermic or endothermic peak was detected in DSC data (not shown in Fig. 1). It should be mentioned that the weight loss was 5 wt% in case of the previously published paper where CuO/CeO_2 catalyst was prepared by co-precipitation with CuO loading of 5.1 wt% [16]. The $CuO–CeO_2$ catalyst after the hydrothermal treatment for 24 h (HT-2 catalyst) showed the decrease in weight loss by 0.5 wt% (Fig. 1) compared to that for 12 h (HT-1 catalyst). From the result of thermogravimetric (TG) analysis, it appears that hydrothermally treated $CuO–CeO_2$ catalyst enhanced the chemical stability compared to the $CuO–CeO_2$ catalyst without hydrothermal treatment. This means that cuprous ion might be well ordered in the lattice of CeO_2 by hydrothermal treatment.

From the TG results of hydrothermally treated $CuO–CeO_2$ catalyst precursor, it is obvious that the calcination temperature should be above 400 °C and therefore the calcination temperatures were selected at 400, 500, 600, 700, and 800 °C, respectively.

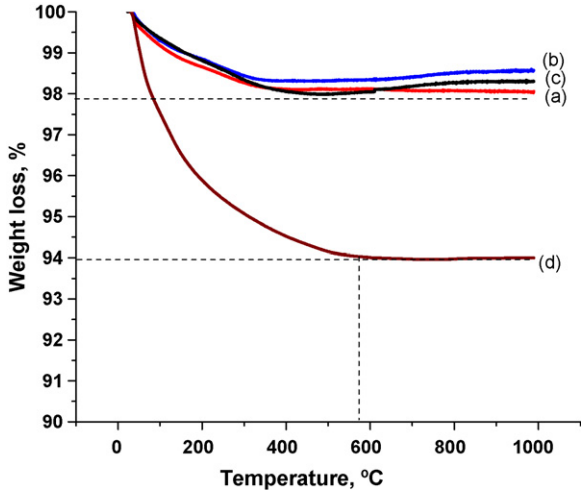

Fig. 1. TG results of (a)–(c) with hydrothermal treatment ((a) HT-1 catalyst, (b) HT-2 catalyst, and (c) HT-3 catalyst) and (d) without hydrothermal treatment.

3.1. Effect of duration time of hydrothermal treatment

The hydrothermally treated catalysts (HT-1 and HT-2) both having the amount of CuO loading of 4.1 wt% were treated for 12 and 24 h, respectively. Table 2 shows the catalytic activity evaluated for selective oxidation of carbon monoxide in terms of residual CO concentration with the hydrothermally treated $CuO–CeO_2$ catalyst prepared at different calcination temperatures.

Table 2
Catalytic activity of HT-1, HT-2 and HT-3 catalyst with various calcination temperatures

Temperature (°C)	Residual CO concentration (ppm) at different calcination temperatures (°C)				
	400[a]	500[a]	600[a]	700[a]	800[a]
HT-1 catalyst					
110	7272	5578	4720	4362	5414
120	6741	4049	3163	2532	3799
130	5977	2677	1776	1103	1980
140	5003	1374	750	290	631
150	3903	507	191	0	54
160	2792	108	0	0	0
170	1845	0	0	0	0
180	1197	0	0	191	33
190	724	216	199	555	447
HT-2 catalyst					
110		4165	4709	4408	5120
120		2553	3347	2880	3544
130		1378	1957	1565	2345
140		602	830	626	1465
150		218	239	137	903
160		44	0	0	572
170		188	0	0	423
180		508	0	0	427
190		796	43	158	606
HT-3 catalyst					
110		5168	5404	5761	5653
120		3502	3817	4059	4051
130		1940	2172	2082	2211
140		947	1032	615	728
150		350	281	11	46
160		29	0	0	0
170		0	0	0	0
180		0	24	78	0
190		0	348	441	422
200		200			

0: not detected in CO analyzer.
[a] Calcination temperature.

Table 3
Catalytic activity of CuO/CeO_2 catalyst (5.1 wt% CuO loading) prepared by co-precipitation method (without hydrotreatment) with various calcination temperatures [16]

Temperature (°C)	Residual CO concentration (ppm) at different calcination temperatures (°C)				
	500[a]	600[a]	700[a]	800[a]	900[a]
110	5790	4297	4985	5683	1468
130	3782	1800	1422	2276	3619
150	2037	626	210	530	1412
160	1481	363	48	286	1076
170	988	268	6	146	850
180	710	314		133	686
190	598			377	558
200	799				958

[a] Calcination temperature.

Both HT-1 and HT-2 catalysts, calcined at 600 and 700 °C, showed a higher activity for selective oxidation of carbon monoxide compared to $CuO–CeO_2$ catalyst prepared by co-precipitation method (Tables 2 and 3).

In the case of HT-2 catalyst, the catalytic activity showed a similar trend with HT-1 catalyst, but the HT-2 catalyst calcined at 800 °C showed a decreased activity for selective oxidation of carbon monoxide. Concerning the catalyst sample hydrotreated for 24 h (HT-2), the desired conversion of CO (below 10 ppm of CO in the outlet gas) achieved at 10 °C higher of the reaction temperature compared to that of HT-1 catalyst. It is obvious that the CuO/CeO_2 catalyst (CuO loading of 5.1 wt%) prepared by co-precipitation (without hydrothermal treatment) in the previous paper [16] has very narrow operating temperature window in order to achieve the output CO concentration of less than 10 ppm. It was achieved only at 170 °C with the catalyst calcined at 700 °C. Similar results were reported by Kim et al. [31] and Cortes et al. [32] with the conventionally prepared CuO/CeO_2 catalyst.

In order to investigate the effect of hydrothermal treatment on the properties of $CuO–CeO_2$ catalyst, several characterization techniques were used. At first, physical properties like BET surface area and pore volume were analyzed using N_2 adsorption–desorption method. Measured physical properties of HT-1 catalyst are summarized in Table 4 and pore size distribution of HT-1 catalyst is shown in Fig. 2. From the results of N_2 adsorption–desorption, it is clear that the pore volume of HT-1 catalyst remained almost same at the calcinations temperature below 600 °C, but the pore volume and BET surface area decreased above 700 °C. This confirms that the sintering of HT-1 catalyst started at 700 °C. However, compared to $CuO–CeO_2$ catalyst prepared by co-precipitation method, the BET surface area of HT-1 catalyst was not enhanced, indicating that the physical properties of $CuO–CeO_2$ catalyst were not improved by hydrothermal treatment.

In order to investigate the reduction characteristics of HT-1 catalyst, TPR experiment was performed in the room temperature to 927 °C range and the TPR profiles are shown in Fig. 3. In the case

Table 4
Physical properties of HT-1 catalyst with various calcination temperatures

Calcination temperature (°C)	S_{BET} (m^2/g)	V (cm^3/g)	D (nm)	S_{BET} (m^2/g)[a]
400	40	0.10	10	
500	39	0.10	11	78
600	35	0.10	11	50
700	30	0.08	13	22
800	13	0.04	13	12

S_{BET}, BET surface area; V, pore volume; D, average pore diameter.
[a] BET surface area of $CuO–CeO_2$ catalyst prepared by co-precipitation method.

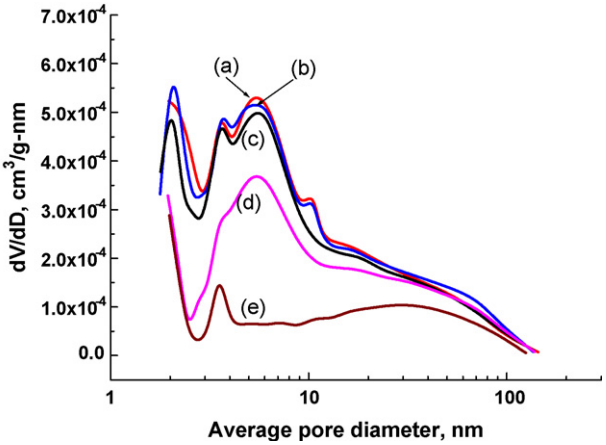

Fig. 2. Pore size distribution of HT-1 catalyst with various calcination temperatures: (a) 400 °C, (b) 500 °C, (c) 600 °C, (d) 700 °C, and (e) 800 °C.

of $CuO–CeO_2$ catalyst prepared by co-precipitation method, three reduction peaks are observed. The two low temperature peaks are due to the reduction of capping oxygen and the high temperature peak is due to the reduction of CeO_2 to Ce_2O_3 [16]. In the case of HT-1 catalyst, four reduction peaks are detected. The high temperature peak is due to the same reason as that in $CuO–CeO_2$ catalyst prepared by co-precipitation method and this peak was not affected by hydrothermal treatment. In addition to that, there are three reduction peaks at low temperature with HT-1 catalyst. The first and second peaks are due to the reduction of capping oxygen and the third peak is a new one. It may be due to the reduction of copper oxide of phase-separated copper. Bozo et al. [33] reported that in the case of ceria–zirconia solid solution, Zr^{4+} cation migrated to the surface at the time of hydrothermal treatment and thus the concentration of zirconium was increased on the surface of ceria–zirconia solid solution. The concentration of cerium was increased in the center of ceria–zirconia solid solution. In the case of $CuO–CeO_2$ catalyst, cuprous ion (Cu^{1+}) migrated to the surface of the catalyst during hydrothermal treatment, and the concentration of copper increased on the surface. Finally, a part of the phase-separated copper and cupric oxide was formed on the surface of catalyst after the calcination of the catalyst.

Most of the copper formed the Cu–Ce–O solid solution and a part of the phase-separated copper and cupric oxide was also formed on the surface of the catalyst when the catalyst was calcined above 800 °C. Liu and Flytzani-Stephonopoulos [34] reported that the amount of copper ion incorporated into the ceria lattice was less than 15 mol%. Although the amount of copper ion was less than 15 mol% in HT-1 catalyst, surface concentration of copper ion was increased and might be phase separated. TPR profiles of HT-2 catalyst which has higher copper loading than HT-1 catalyst are presented in Fig. 4. The TPR results of HT-2 catalyst were of the same pattern with HT-1 catalyst, but the area of the third peak increased, suggesting that the amount of exposed cupric oxide increased, compared to the HT-1 catalyst. The cupric oxide formed in the hydrothermally treated $CuO–CeO_2$ catalyst had a different interactions with catalyst because the third peak in TPR profiles of HT-1 and HT-2 catalysts showed a different trends with increasing calcination temperature. In the case of HT-2 catalyst, the position of the third peak remained constant till the calcination temperature of 600 °C and the peak was shifted to a higher temperature region when the catalyst was calcined at 700 °C. However, in the case of HT-1 catalyst, the position of the third peak was slightly shifted to a lower temperature with the increasing calcination temperature from 500 to 600 °C and then shifted to a higher temperature when the catalyst was calcined at 700 °C.

3.2. Effect of CuO loading with the same duration time of hydrothermal treatment

Table 2 also shows the comparison performance of two types of CuO/CeO_2 catalysts (HT-1 and HT-3 with same duration time for hydrothermal treatment but having different amounts of CuO loading 4.1 and 5.6 wt%, respectively). On the other hand, HT-3 catalyst showed the superior activity with the catalyst calcined at 500 °C and the operating temperature window was also widened by 10 °C. From the activity data, it is clear that the catalytic activity was affected by the hydrothermal condition and the loading amount of copper in $CuO–CeO_2$ catalyst.

To check the chemical structure of hydrothermally treated $CuO–CeO_2$ catalyst, XRD analysis of HT-1 and HT-3 catalysts was carried out and the XRD patterns of HT-1 catalyst are shown in Fig. 5. In all HT-1 catalysts, XRD peaks for CeO_2 only was detected, but the XRD peaks for copper oxide such as cupric oxide or cuprous oxide were not observed (generally XRD characteristic peaks of CuO and Cu_2O appear in the region of 35–40° [35]). The XRD peak for cupric oxide was detected in only hydrothermally treated $CuO–CeO_2$ catalyst which is calcined at 800 °C. HT-3 catalyst also showed the same XRD results as HT-1 catalyst (not shown in figure). The XRD results of hydrothermally treated $CuO–CeO_2$

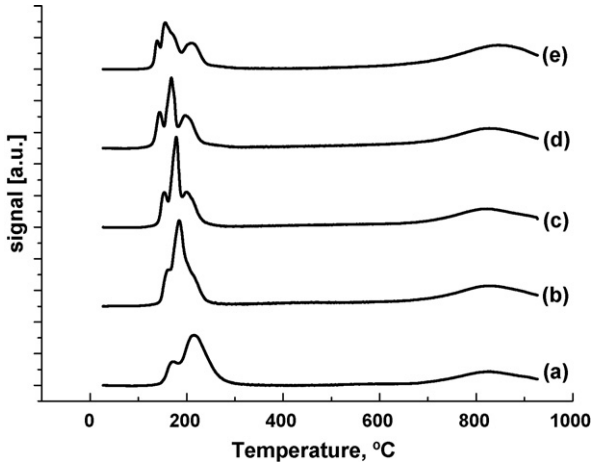

Fig. 3. TPR profiles of HT-1 catalyst with various calcination temperatures: (a) 400 °C, (b) 500 °C, (c) 600 °C, (d) 700 °C, and (e) 800 °C.

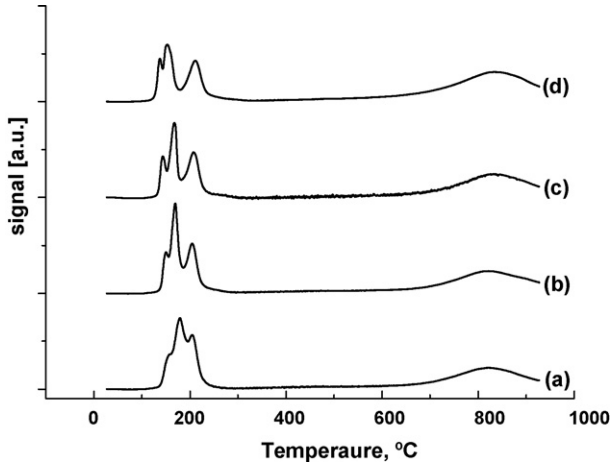

Fig. 4. TPR profiles of HT-2 catalyst with various calcination temperatures: (a) 500 °C, (b) 600 °C, (c) 700 °C, and (d) 800 °C.

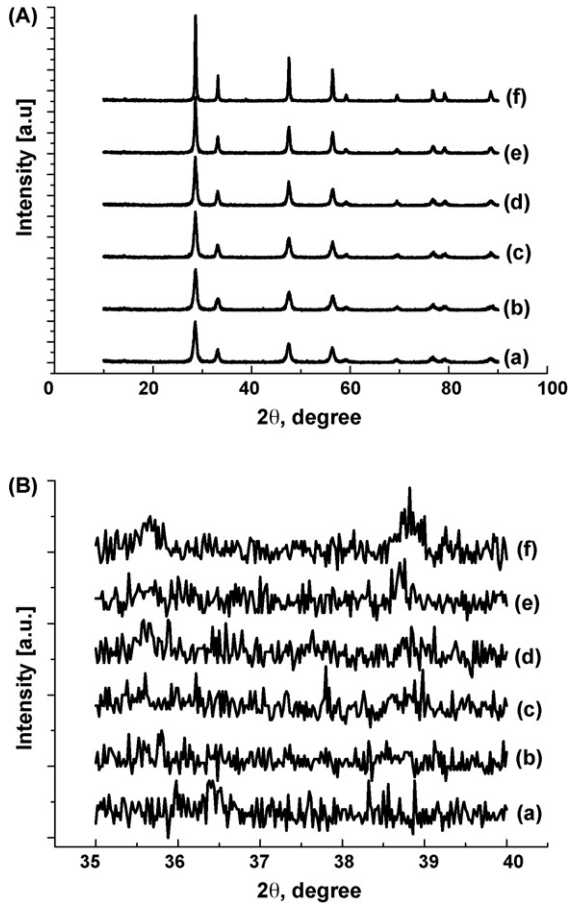

Fig. 5. (A) XRD patterns of HT-1 catalyst with various calcination temperatures: (a) without calcination, (b) 400 °C, (c) 500 °C, (d) 600 °C, (e) 700 °C, and (f) 800 °C. (B) The enlarged view of XRD patterns in the scan range of 35–40° of HT-1 catalyst with various calcination temperatures: (a) without calcination, (b) 400 °C, (c) 500 °C, (d) 600 °C, (e) 700 °C, and (f) 800 °C.

catalyst are in the same trend with the increase of calcination temperature with CuO–CeO_2 catalyst prepared by co-precipitation method. This suggests that all hydrothermally treated CuO–CeO_2 catalyst resulted in the formation of a Cu–Ce–O solid solution-like CuO–CeO_2 catalyst prepared by co-precipitation method [16] and phase separation with a part of the copper when calcined at 800 °C, followed by the formation of cupric oxide on the surface of the catalyst.

To check the oxidation state of copper in the HT-1 catalyst, XPS analysis was carried out and the results are summarized in Table 5. The binding energy of copper in CuO–CeO_2 catalyst prepared by co-precipitation method is 932.0 eV, suggesting that the oxidation state of copper is 1+ and it represents Cu_2O. On the other hand, in case of HT-1 and HT-3 catalyst, the binding energy of copper is between 932.7 and 933.7 eV, except for the HT-1 catalyst calcined at 500 °C. Copper was not phase separated in the HT-1 catalyst

Table 5
The binding energy of copper in the HT-1 and HT-3 catalyst

Calcination temperature (°C)	Binding energy of HT-1 (eV)	Binding energy of HT-3 (eV)
500	932.0	933.0
600	932.7	933.2
700	933.2	933.0
800	933.2	933.7

Table 6
CO uptakes of hydrothermal-treated CuO–CeO_2 catalyst prepared at various calcination temperature

Catalyst	Calcination temperature (°C)	CO uptake ($\times 10^5$ mol/g)		
		Reversible	Irreversible	Total
CuO–CeO_2[a]	700	3.62	5.54	9.15
HT-1	400	2.19	4.29	6.47
	500	2.77	4.29	7.05
	600	3.66	7.32	10.98
	700	4.78	9.33	14.11
	800	2.90	6.43	9.33
HT-2	500	3.62	4.91	8.53
	600	4.33	7.68	12.01
	700	5.89	8.48	14.38
	800	5.49	6.38	11.88
HT-3	500	4.46	13.53	17.99
	600	4.42	13.13	17.54
	700	4.15	12.50	16.65
	800	2.05	5.76	7.81

[a] CuO–CeO_2 catalyst prepared by co-precipitation method.

which is calcined at 500 °C. Therefore, cupric oxide was not formed on the surface of catalyst. However, in the other cases, a part of the copper was phase separated and formed cupric oxide on the surface of the catalyst and thus the binding energy of copper in catalyst was shifted to a higher value with increasing amount of cupric oxide on the surface of catalyst. In between the HT-1 and HT-3 catalysts, the binding energy of copper was shifted to a higher value in the case of HT-3 catalyst indicating that the amount of cupric oxide on the surface of catalyst was higher than that of HT-1 catalyst. The XPS results of HT-1 catalyst coincided with the TPR results of HT-1 catalyst.

In order to calculate the amount of carbon monoxide chemisorbed on the surface of the hydrothermally treated CuO–CeO_2 catalyst, CO chemisorption analysis was carried out and the results are summarized in Table 6. In the case of CuO–CeO_2 catalyst prepared by co-precipitation method, the amount of carbon monoxide uptake decreased with increasing calcination temperature and the trend coincided with the physical properties of the catalyst such as BET surface area, pore volume, and average pore diameter [16]. However, in the case of HT-1 and HT-2 catalysts, the amount of carbon monoxide uptakes showed a volcano curve with increase of calcination temperature and the hydrothermally treated catalyst calcined at 700 °C had the largest amount of carbon monoxide uptake. On the other hand, the amount of carbon monoxide uptake decreased with increasing calcination temperature in the case of HT-3 catalyst. These results were well matched with the results of CuO–CeO_2 catalyst prepared by co-precipitation method. Comparing the amounts of carbon monoxide uptakes in CuO–CeO_2 catalysts prepared by hydrothermal treatment and co-precipitation method, it is observed that the amount of CO uptake is always higher in the case of the hydrothermally treated catalyst. However, it was not possible to find any correlation between the catalytic activity and the chemical properties which was calculated from the results of CO chemisorption.

4. Conclusions

In this study, hydrothermally treated CuO–CeO_2 catalyst was prepared and evaluated for selective oxidation of CO in a typical gas composition from methanol steam reforming reaction. The catalytic activities for the selective oxidation of carbon monoxide over hydrothermally treated CuO–CeO_2 catalyst were increased and the temperature window was widened. The physical proper-

ties such as BET surface area, pore volume and average pore diameter were not improved by the hydrothermal treating condition, but the chemical stability of the catalyst was enhanced. During the hydrothermal treatment, cuprous ion migrated to the surface of the $CuO–CeO_2$ catalyst and cupric oxide was formed on the surface of catalyst during calcination. Phase separation of copper in the catalyst with calcination temperature showed the same trend as in the case of $CuO–CeO_2$ catalyst prepared by co-precipitation method. After ageing of $CuO–CeO_2$ catalyst under hydrothermal condition for a long time (HT-2 catalyst), the surface concentration of copper was increased and the amount of cupric oxide having bulk properties was increased. In the case of HT-3 catalyst in which the CuO loading was increased, the amount of phase-separated copper might be decreased because the surface concentration of copper in the $CuO–CeO_2$ catalyst was increased.

Acknowledgements

This work was financially supported by Korea Institute of Science and Technology, and by the ERC program of MOST/KOSEF (Grant No. R11-2002-102-00000-0).

References

[1] R.A. Lemons, J. Power Sources 29 (1990) 251.
[2] H. Igarashi, T. Fujino, M. Watanabe, J. Electroanal. Chem. 391 (1995) 119.
[3] H.F. Oetjen, V.M. Schmidt, U. Stimming, F. Trila, J. Electrochem. Soc. 143 (1996) 3838.
[4] M. Watanabe, H. Igarashi, T. Fujino, Electrochemistry 67 (1999) 1194.
[5] M. Watanabe, Y. Zhu, H. Uchida, J. Phys. Chem. B 104 (2000) 1762.
[6] H. Igarashi, T. Fujino, Y. Zhu, H. Uchida, M. Watanabe, Phys. Chem. Chem. Phys. 3 (2001) 306.
[7] S.H. Oh, R.M. Sinkevitch, J. Catal. 142 (1993) 254.
[8] M.J. Kahlich, H.A. Gasteiger, R.J. Behm, J. Catal. 171 (1997) 93–105.
[9] H. Igarashi, H. Ushida, M. Suzuki, Y. Sasaki, M. Watanabe, Appl. Catal. A: Gen. 159 (1997) 159.
[10] G.K. Bethke, H.H. Kung, Appl. Catal. A: Gen. 194 (2000) 43.
[11] R.J.H. Grisel, B.E. Nieuwenhuys, J. Catal. 199 (2001) 48–59.
[12] M.J. Kahlich, A. Gasteiger, R.J. Behm, J. Catal. 182 (1999) 430.
[13] W.-S. Shin, C.-R. Jung, J. Han, S.-W. Nam, T.-H. Lim, S.-A. Hong, H.-I. Lee, J. Ind. Eng. Chem. 10 (2004) 33.
[14] G. Avgouropoulos, T. Ioannides, Ch. Papadopoulou, J. Batista, S. Hocevar, H.K. Matralis, Catal. Today 75 (2002) 157.
[15] G. Avgouropoulos, T. Ioannides, H. Matralis, J. Batista, S. Hocevar, Catal. Lett. 73 (2001) 33.
[16] C.R. Jung, J. Han, S.W. Nam, T.-H. Lim, S.-A. Hong, H.-I. Lee, Catal. Today 93–95 (2004) 183.
[17] E. Simsek, S. Ozkara, A.E. Aksoylu, Z.I. Onsan, Appl. Catal. A: Gen. 316 (2007) 169.
[18] K. Omata, Y. Kobayashi, M. Yamada, Catal. Commun. 8 (2007) 1.
[19] D. Gamarra, A. Hornes, Zs. Koppany, Z. Schay, G. Munuera, J. Soria, A. Martinez-Arias, J. Power Sources 169 (2007) 110.
[20] J.L. Ayastuy, M.P. Gonzalez-Marcos, J.R. Gonzalez-Velasco, M.A. Gutierrez-Ortiz, Appl. Catal. B: Environ. 70 (2007) 532.
[21] W.-S. Lee, B.-Z. Wan, C.-N. Kuo, W.-C. Lee, S. Cheng, Catal. Commun. 8 (2007) 1604.
[22] O. Pozdnyakova, D. Teschner, A. Wootsch, J. Kröhnert, B. Steinhauer, H. Sauer, L. Toth, F.C. Jentoft, A. Knop-Gericke, Z. Paál, R. Schlögl, J. Catal. 237 (2006) 1.
[23] I.H. Son, J. Power Sources 159 (2006) 1266.
[24] G. Avgouropoulos, J. Papavasiliou, T. Tabakova, V. Idakiev, T. Ioannides, Chem. Eng. J. 124 (2006) 41.
[25] J.L. Ayastuy, M.P. Gonzalez-Marcos, A. Gil-Rodrıguez, J.R. Gonzalez-Velasco, M.A. Gutierrez-Ortiz, Catal. Today 116 (2006) 391.
[26] H.L. Barnes (Ed.), Geochemistry of Hydrothermal Ore Deposits, 2nd ed., Wiley, New York, 1979.
[27] C.R. Veal, Fine Powders, Preparation, Properties and Uses, Wiley, New York, 1972.
[28] K. Yanagisawa, H. Kanai, Y. Yamashita, Jpn. J. Appl. Phys. 36 (1997) 6031.
[29] E.P. Barrett, L.G. Joyner, P.P. Halenda, J. Am. Chem. Soc. 73 (1951) 373.
[30] C.R. Jung, A. Kundu, S.W. Nam, H.-I. Lee, Appl. Catal. A: Gen. 331 (2007) 112.
[31] K.-Y. Kim, J. Han, S.W. Nam, T.-H. Lim, H.-I. Lee, Catal. Today 131 (2008) 431.
[32] A. G.-Cortes, Y. Marquez, J. A.-Alatorre, G. Diaz, Catal. Today 133–135 (2008) 743.
[33] C. Bozo, F. Gaillard, N. Guilhaume, Appl. Catal. A: Gen. 220 (2001) 69.
[34] W. Liu, M. Flytzani-Stephonopoulos, J. Catal. 153 (1995) 304.
[35] JCPD file: 45-0937.